Supporting Information

Diradical-Featured N-Arene Croconaine-Based Nanoagent for Synergistic Photodynamic/Photothermal Tumor Therapy

Yiru Tang,‡[a, b] Xiaoyu Zhu,‡[a] Yating Zeng,[a] Wanying Li,[a] Na Hao,[a] Ji Lu,[a] Bowen Lei,[a] Yao Jian,*[a] and Lin Yang*[a]

[a] Green Pharmaceutical Technology Key Laboratory of Luzhou City, Central Nervous System Product Research and Development Key Laboratory of Sichuan Province, School of Pharmacy, Southwest Medical University, Luzhou 646000, PR China
E-mail: jianyao@swmu.edu.cn yanglinyjl@swmu.edu.cn.

[b] Department of Pharmacy, Wusheng People's Hospital, Guangan 638400, PR China

‡ These authors contributed equally to this work.

Table S1 Photothermal properties of croconaine-based photothermal agents with different structural types.

Croconaine dyes		PCE	Treatment methods	References
C-arene CR	CR780	54.49%	PTT	1
	TCR	77%	PDT/PTT	2
	CCQ	62.9%	PTT	3
	CR880	58%	PTT	4
	DRM	68%	PTT	5
	CR-DPA-T	72%	PTT	6
C-arylidene CR	Croc770	32.0%	PTT	7
	Croc815	34.7%	PTT	7
	CR760	45.37%	PTT	8
	CR-630	46.1%	PTT	9
	CR1045	84%	PTT	10
N-arene CR	CR-$(DPA)_2$OMe	85.05%	water evaporation and antibacterial effect	11
	CR620	**41.12%**	**PDT/PTT**	**this work**

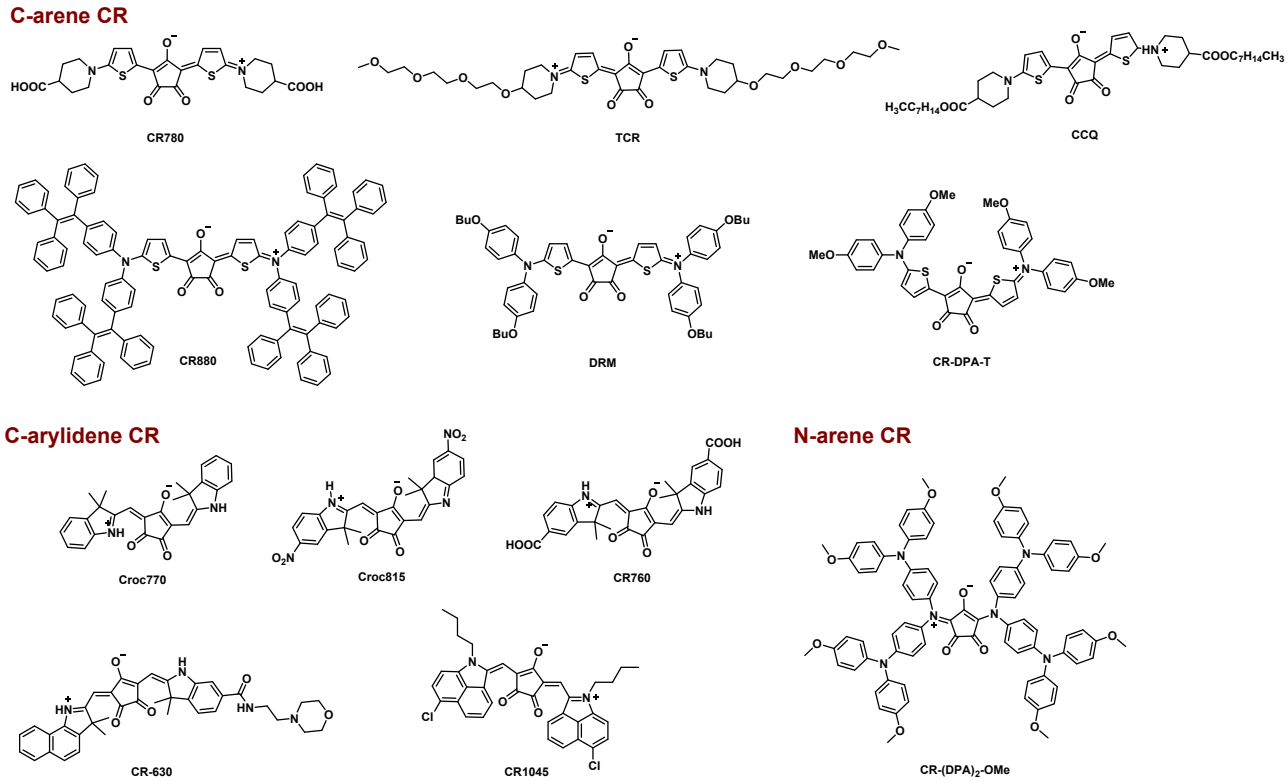

Figure S1. Chemical structures of the croconaine dyes mentioned in Table S1.

Table S2 Comparison of irradiation parameters between this work and representative literature.

Power density (W/cm^2)	Irradiation time (min)	Energy dose (J/cm^2)	Reference
1	**1**	**60**	**this work**
0.7	5	210	12
0.8	6	288	13
0.7	10	420	10
1.5	5	450	14
1	10	600	5, 15-17

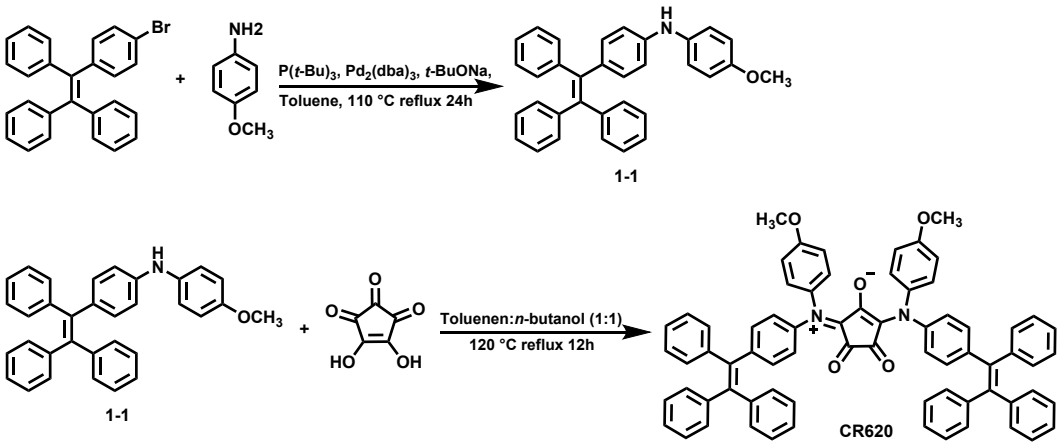

Figure S2. Synthetic routes of **1-1** and CR620.

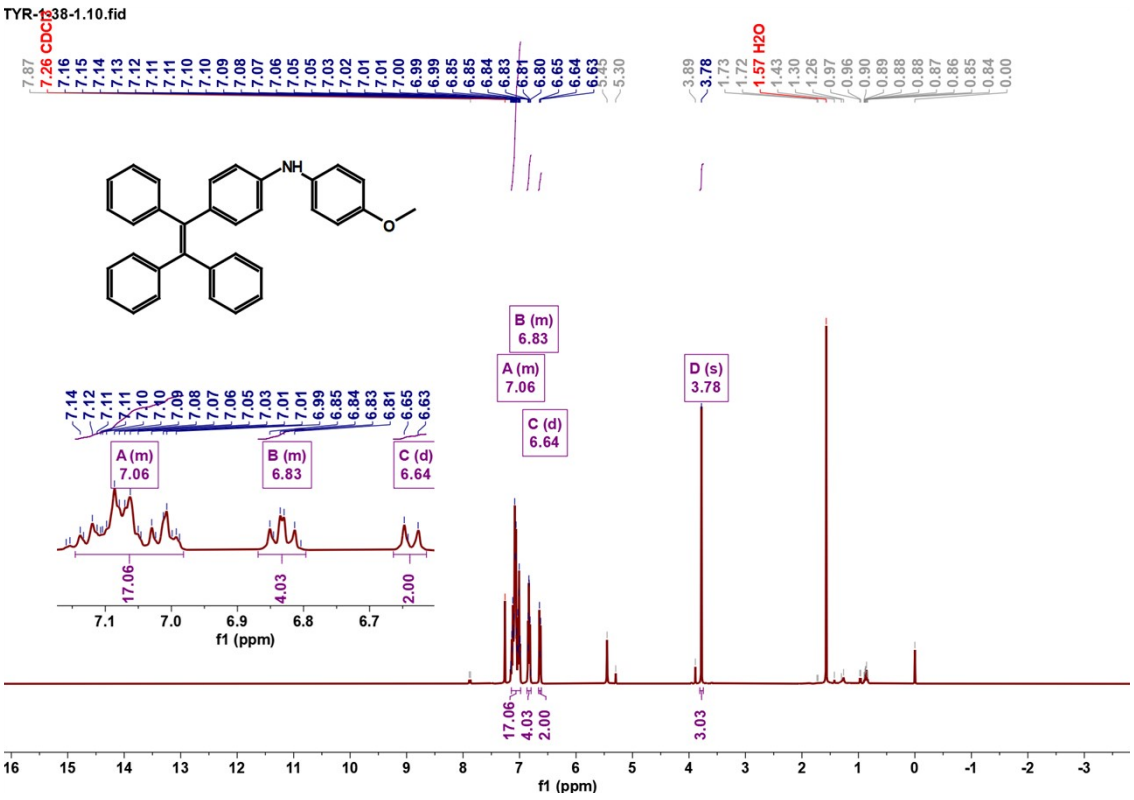

Figure S3. [1]H NMR spectrum of **1-1**.

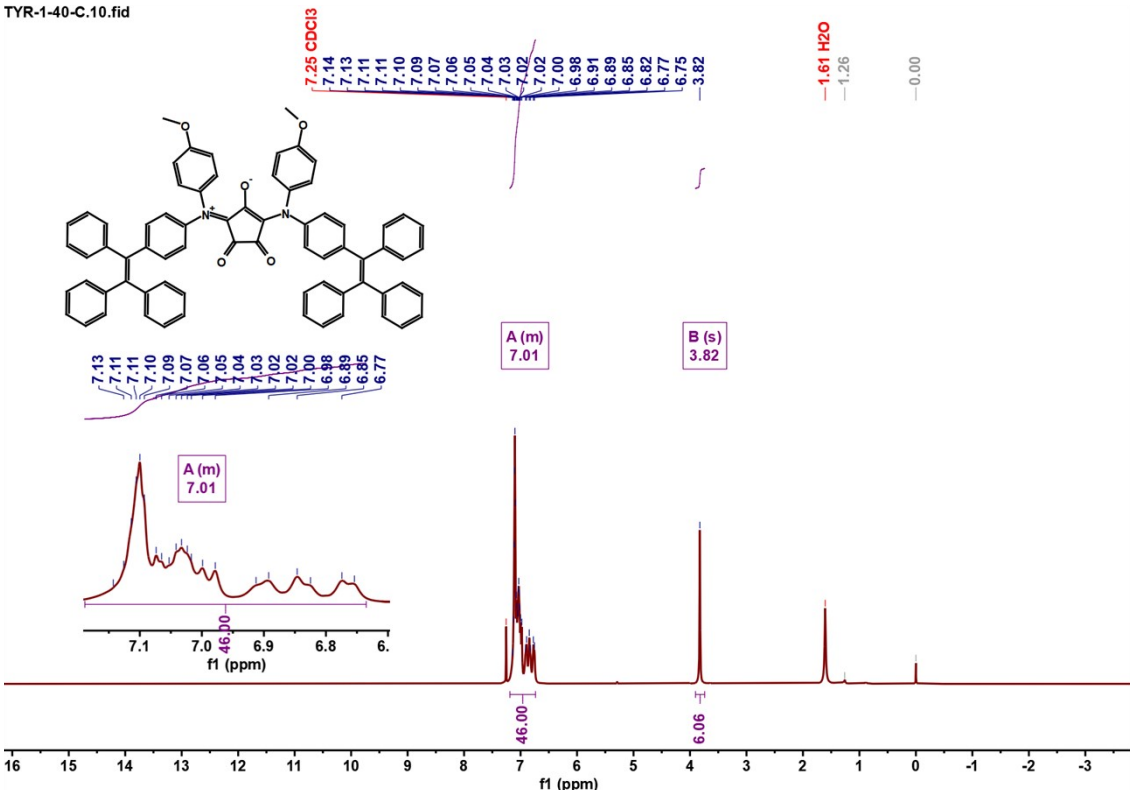

Figure S4. [1]H NMR spectrum of CR620.

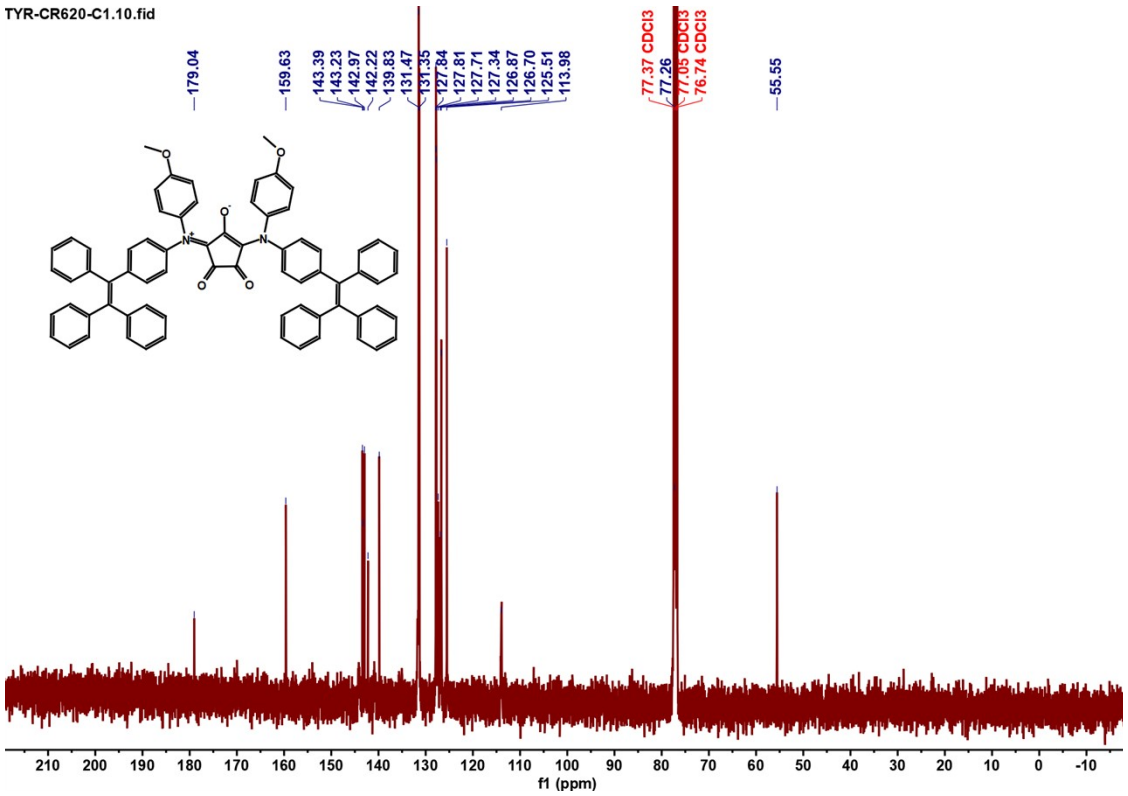

Figure S5. [13]C NMR spectrum of CR620.

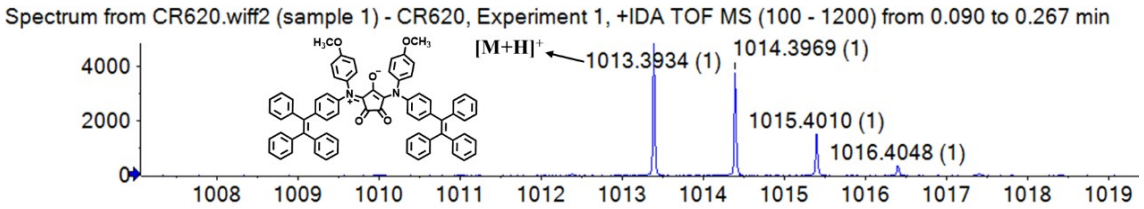

Figure S6. MS of CR620.

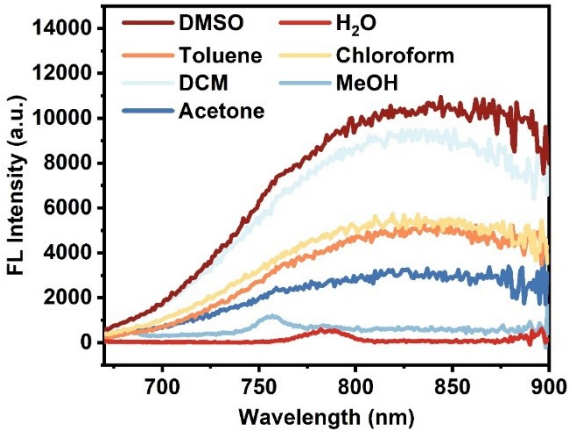

Figure S7. Fluorescence emission spectra of CR620 in different solvents.

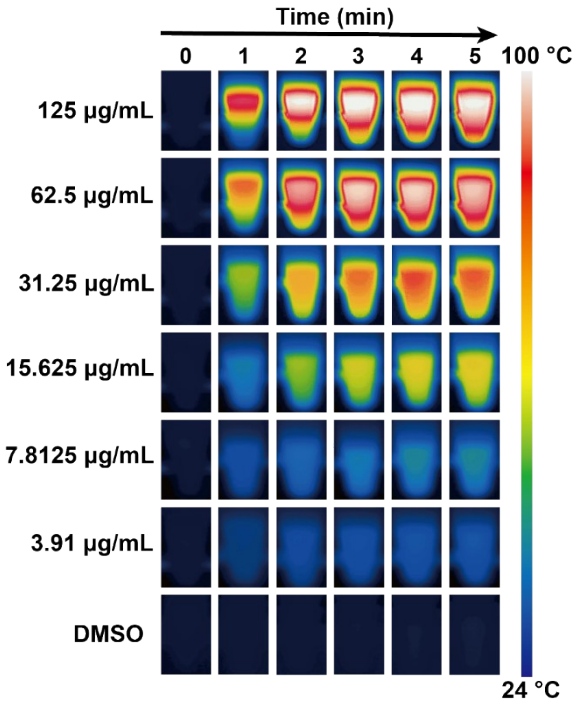

Figure S8. Thermal infrared images of CR620 dimethyl sulfoxide solution at different concentrations upon irradiation of a 660 nm CW laser (1.0 W/cm^2).

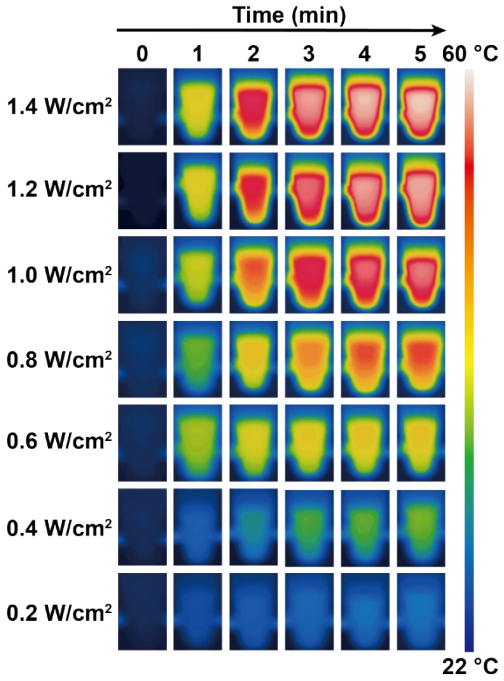

Figure S9. Thermal infrared images of CR620 dimethyl sulfoxide solution (7.8125 μg/mL) upon irradiation of a 660 nm CW laser with different power densities.

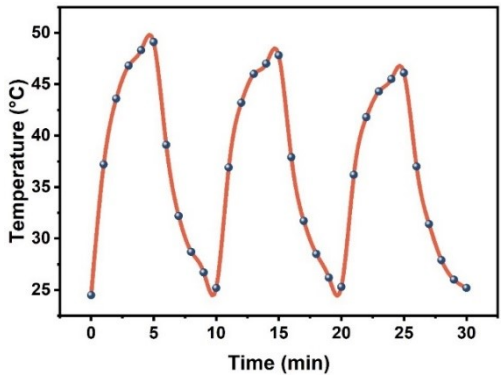

Figure S10. Photothermal stability test of CR620 dimethyl sulfoxide solution (7.8125 μg/mL) during three irradiation cycles.

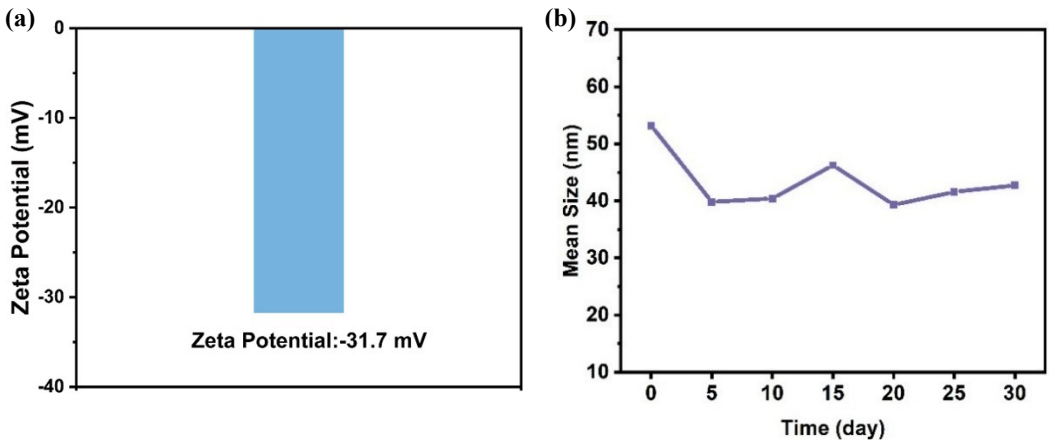

Figure S11. (a) Zeta potential of CR620 NPs; (b) Size stability of CR620 NPs in water during 30 days.

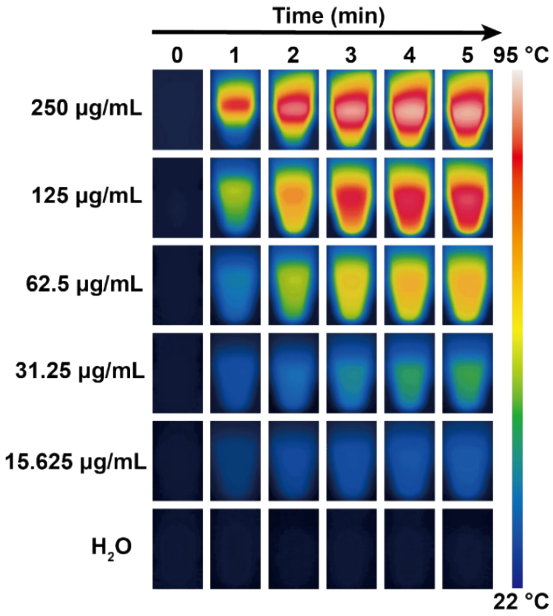

Figure S12. Thermal infrared images of CR620 NPs with different concentrations upon irradiation of a 660 nm CW laser (1.0 W/cm^2).

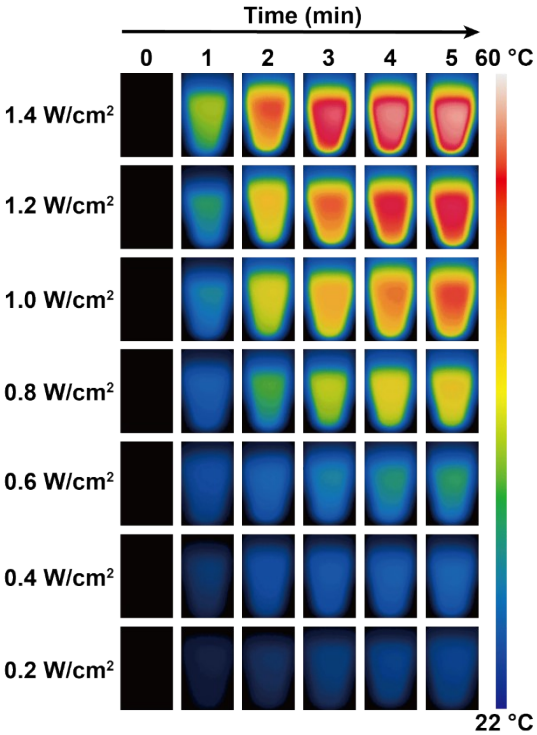

Figure S13. Thermal infrared images of CR620 NPs (31.25 μg/mL) irradiated by a 660 nm CW laser with different power densities.

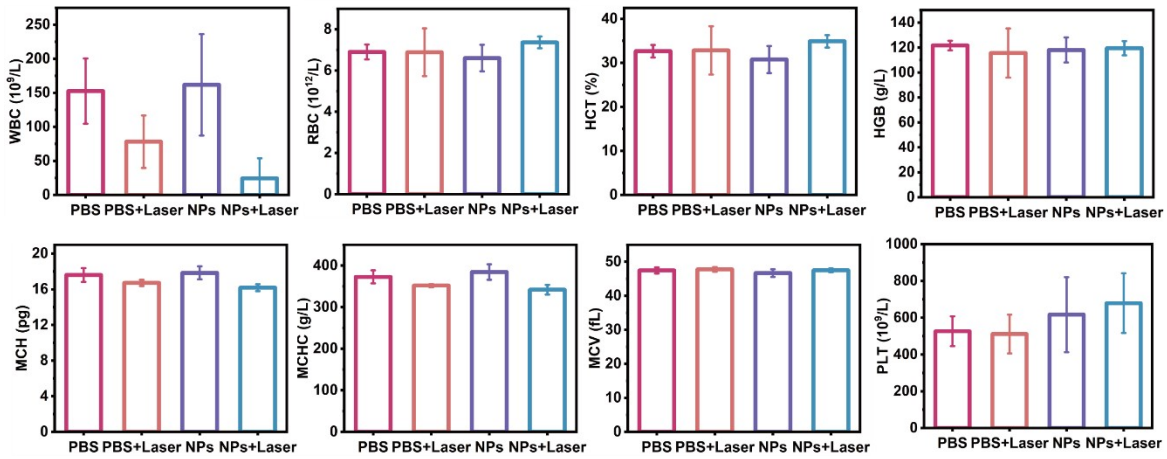

Figure S14. Blood routine examination for the mice (the normal reference ranges for these parameters: WBC, 0.8-10.6 × 10^9/L; RBC, 6.5-11.5 × 10^{12}/L; HCT, 35-55%; HGB, 110-165 g/L; MCH, 13-18 pg; MCHC, 300-360 g/L; MCV, 41-55 fL; PLT, 400-1600 × 10^9/L).

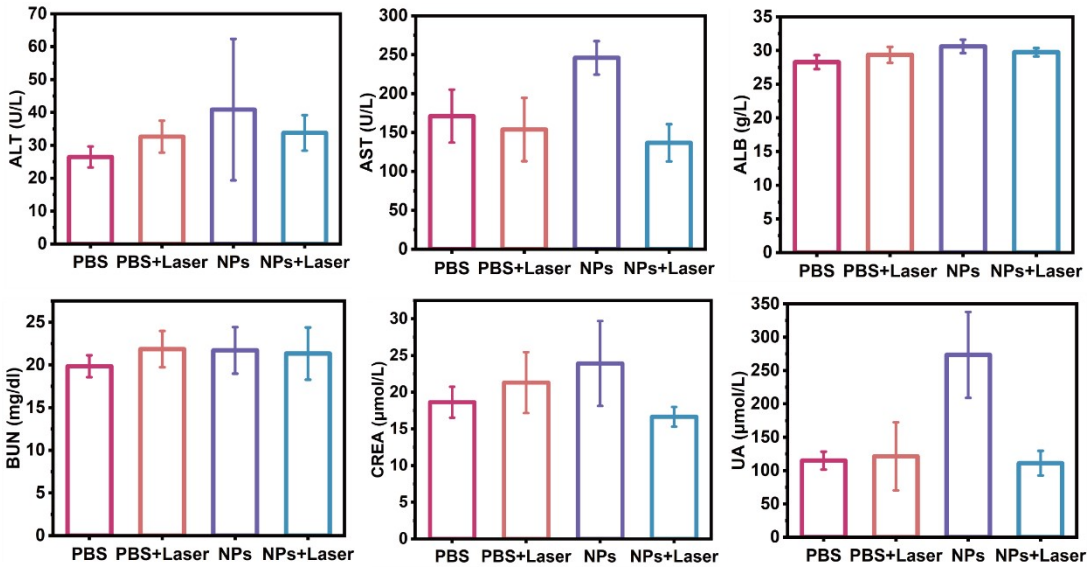

Figure S15. Blood biochemistry analysis for the mice (the normal reference ranges for these parameters: ALT, 10.06-96.47 U/L; AST, 36.31-235.48 U/L; ALB, 21.22-39.15 g/L; BUN, 10.81-34.74 mg/dl; CREA, 10.91-85.09 μmol/L; UA, 44.42-224.77 μmol/L).

2. Photothermal Conversion Efficiency Calculation[5]

To calculate the PCE of CR620 and CR620 NPs, the following protocol was implemented. First, CR620 and CR620 NPs were dissolved in dimethyl sulfoxide (DMSO) or water to prepare solutions of varying concentrations, ensuring complete dissolution. Subsequently, 200 μL of each sample was transferred to an EP tube. The sample was irradiated with a 660 nm laser for 5 min, during which temperature was recorded at 60 s intervals using a thermal infrared camera. After laser cessation, the sample was allowed to cool naturally to room temperature, with temperature monitored until stabilization. Using CR620 DMSO solution as an example, the PCE was calculated via the following equation 1:

$$\eta = \frac{hs(T_{max} - T_{surr}) - Q_{dis}}{I\left(1 - 10^{-A_{660}}\right)}$$

where h represents the heat transfer coefficient, s is the surface area of the EP tube, T_{max} is the maximum temperature achieved by laser irradiation of the sample, T_{surr} is the ambient temperature of the environment set at 22 °C, Q_{dis} is the heat dissipation from solvent and EP tube absorption, I is the incident laser power (1.0 W/cm^2), and A_{660} is the absorbance of CR620 DMSO solution (7.8125 μg/mL) at 660 nm.

The value hs was calculated using the following equation 2:

$$hs = \frac{m_D C_D}{\tau_S}$$

where τ_s is the time constant of the sample system, m_D and c_D are the mass (0.22 g) and heat capacity (1.95 kJ/(kg·°C)) of DMSO respectively.[18]

The value τ_s can be derived from the following equation 3:

$$\tau_s = \frac{t}{-\ln\theta}$$

where t is the time elapsed after laser irradiation ceases and θ is normalized temperature decay parameter and calculated using the following equation 4:

$$\theta = \left(\frac{T_{RT} - T_{surr}}{T_{max} - T_{surr}}\right)$$

where T_{RT} is the sample temperature at time t.

Q_{dis} was calculated using the following equation 5:

$$Q_{dis} = \frac{m_D C_D\left(T_{max}(DMSO) - T_{surr}\right)}{\tau_s(DMSO)}$$

References

1. L. Tang, F. Zhang, F. Yu, W. Sun, M. Song, X. Chen, X. Zhang and X. Sun, *Biomaterials*, 2017, **129**, 28-36.
2. E. Pang, R. Huang, S. Zhao, K. Yang, B. Li, Q. Tan, S. Tan, M. Lan, B. Wang and X. Song, *J. Mater. Chem. B*, 2022, **10**, 9848-9854.
3. W. Wang, J. Yu, Y. Lin, M. Li, Y. Pan, Y. He, L. Liu, X. Meng, Z. Lv, K. Jin, S. Che, X. Mou and Y. Cai, *Biomater. Adv.*, 2023, **149**, 213418.
4. N. Liu, P. O'Connor, V. Gujrati, P. Anzenhofer, U. Klemm, K. Kleigrewe, M. Sattler, O. Plettenburg and V. Ntziachristos, *Nanophotonics*, 2022, **11**, 4637-4647.
5. X. Li, D. Zhang, C. Yin, G. Lu, Y. Wan, Z. Huang, J. Tan, S. Li, J. Luo and C. S. Lee, *ACS Appl. Mater. Interfaces*, 2021, **13**, 15983-15991.
6. Y. Dong, P. Xia, X. Xu, J. Shen, Y. Ding, Y. Jiang, H. Wang, X. Xie, X. Zhang, W. Li, Z. Li, J. Wang and S. C. Zhao, *J. Nanobiotechnol.*, 2023, **21**, 442.
7. S. Li, K.-H. Lui, X. Li, X. Fang, W.-S. Lo, Y.-J. Gu and W.-T. Wong, *ACS Appl. Bio Mater.*, 2021, **4**, 4152-4164.

8. N. Liu, P. O'Connor, V. Gujrati, D. Gorpas, S. Glasl, A. Blutke, A. Walch, K. Kleigrewe, M. Sattler, O. Plettenburg and V. Ntziachristos, *Adv. Healthc. Mater.*, 2021, **10**, 2002115.
9. P. D. You, C. R. Ouyang, F. Lu, C. Zeng, H.-D. Cai, G.-S. Shi, L. Liu and C.-Q. Zhou, *J. Photochem. Photobiol. B: Biol.*, 2023, **245**, 112748.
10. J. Li, X. Su and N. Liu, *Sensors Actuators B: Chem.*, 2024, **408**, 1355535.
11. L. Yang, G. Wang, Y. Zhang, J. Zhou, R. Wu, C. Qin, Q. Chang, C. Zhang, S. Duan and X. Gu, *Angew. Chem. Int. Ed.*, 2025, **64**, e202508821.
12. X. Chen, X. Ma, G. Yang, G. Huang, H. Dai, J. Yu and N. Liu, *ACS Appl. Mater. Interfaces*, 2024, **16**, 12332-12338.
13. Y. Dong, H. Wang, X. Zhang, Y. Ding, Y. Zou, J. Wang, S.-C. Zhao and Z. Li, *J. Nanobiotechnol.*, 2024, **22**, 481.
14. Y. Chen, L. Liu, L. Yu, Y. Kang, S. Yao, D. Wu, J. Xu, X. Mou and Y. Cai, *Chem. Eng. J.*, 2024, **488**, 150907.
15. P. You, F. Lu, C. Ouyang, J. Yu, J. González-García, J. Song, W. Ni, J. Wang, C. Yin and C.-Q. Zhou, *ACS Appl. Mater. Interfaces*, 2024, **16**, 46066-46078.
16. C. Ouyang, J. Yu, H. Teng, G. Ou, B. Lu, X. Zhang, H. Xie and C.-Q. Zhou, *J. Colloid Interface Sci.*, 2026, **702**, 139005.
17. X. Kong, J. Liang, M. Lu, K. Zhang, E. Zhao, X. Kang, G. Wang, Q. Yu, Z. Gan and X. Gu, *Adv. Mater.*, 2024, **36**, 2409041.
18. Ferdinandus, W. L. L. Tan, J. R. Tan, H. K. Lee, Q. Zhu, E. Ye and C.-L. K. Lee, *Chem. Asian J.*, 2024, **19**, e202400328.